AIAA JOURNAL
Vol. 45, No. 2, February 2007

Experimental and Analytical Estimation of Loss Factors by the Power Input Method

Wanbo Liu* and Mark S. Ewing†
University of Kansas, Lawrence, Kansas 66045

DOI: 10.2514/1.24772

The system loss factor of sandwich panels with different configurations of constrained layer damping treatments is estimated both experimentally and analytically using the power input/injection method over a broad frequency range. Results of the experimental power input method are compared with results from other experimental methods. A new analytical power input method is proposed for evaluating the loss factor of built-up structures, based on a finite element model with assigned properties of the constituents. The new analytical power input method is evaluated by comparison with the commonly used modal strain energy method. Instead of making an approximate correction of the constant material properties, this analytical power input method directly takes into account the frequency-dependent material properties of the viscoelastic material, using the MSC/NASTRAN direct frequency-response solution. Results of experimental and analytical methods are presented, compared, and discussed. It is shown that all three currently available experimental methods yield consistent results and that both the analytical power input method and the modal strain energy method yield results consistent with the experimental power input method.

Nomenclature

E_D	=	energy dissipated per cycle during period T (real)
E_K	=	kinetic energy (real)
$E^{(r)}$	=	total strain energy of the natural mode r (real)
$E_i^{(r)}$	=	strain energy in material i when the structure deforms at the natural mode r (real)
E_S	=	strain energy (real)
E_{Tot}	=	total mechanical (reversible/vibrational) energy (real)
$F_f(t)$	=	force at the driving point (complex)
$F_f(\omega)$	=	Fourier transform of $F_f(t)$ (complex)
f_r	=	rth modal frequency calculated with the core shear modulus as $G_{2,\text{ref}}$ (real)
G_1, G_3	=	shear modulus of the elastic layers (real)
$G_2(f)$	=	real part of the shear modulus of the viscoelastic layer (real)
$G_2'(f)$	=	imaginary part of the shear modulus of the viscoelastic layer (real)
$G_{2,\text{ref}}$	=	real part of the shear modulus of the viscoelastic layer used in normal modes calculation (real)
g	=	overall structural damping (real)
g_{ref}	=	reference element damping (real)
m_i	=	mass of portion i (real)
P_D	=	dissipated power, $P_D = (1/T) \cdot E_D = [\omega/(2 \cdot \pi)] \cdot E_D$ (real)
P_I	=	input power (real)
$R_{F_f V_f}(0)$	=	cross correlation between the driving point force and velocity (real)
$R_{V_i V_i}(0)$	=	autocorrelation of the velocity at point i (real)
$S_{F_f F_f}(\omega)$	=	power spectrum density of the driving point force (real)
$S_{F_f V_f}(\omega)$	=	cross power spectrum density between the driving point force and velocity (real)
$S_{V_i V_i}(\omega)$	=	power spectrum density of the velocity at point i (real)
$TI(f)$	=	tabular function representing the imaginary part of the complex moduli (real)
$TR(f)$	=	tabular function representing the real part of the complex moduli (real)
$V_f(t)$	=	velocity at the driving point (complex)
$Y_{ff}(\omega)$	=	mobility (velocity/force) of the driving point (real)
$Y_{if}(\omega)$	=	mobility (velocity/force) between the driving point f and the point i (complex)
$\Delta\omega$	=	bandwidth (real)
η	=	system loss factor (real)
η_i	=	material loss factor for material i (real)
$\eta^{(r)}$	=	system's modal loss factor at the rth mode by the modal strain energy method (real)
$\eta^{(r)'}$	=	system's adjusted modal loss factor for the rth mode by the modal strain energy method (real)
η_{vem}	=	material loss factor for the viscoelastic material (real)
ρ	=	density (real)
ω	=	circular frequency (real)
ω_C	=	center frequency of the frequency band $[\omega_1, \omega_2]$ (real)
ω_1	=	lower limit of the frequency band (real)
ω_2	=	upper limit of the frequency band (real)
$\bar{\ }$	=	time average

Presented as Paper 2233 at the 47th AIAA/ASME/ASCE/AHS/ASC Structures, Structural Dynamics, and Materials Conference, Newport, RI, 1–4 May 2006; received 23 April 2006; revision received 8 September 2006; accepted for publication 4 October 2006.

*Graduate Research Assistant, Department of Aerospace Engineering; wbliu@ku.edu. Student member AIAA.

†Associate Professor, Department of Aerospace Engineering, University of Kansas, Lawrence, Kansas 66045; mewing@ku.edu. Senior Member AIAA.

I. Introduction

In structural design and/or optimization, knowledge about damping is essential. However, due to the complexity of the dynamic interaction of system components, the determination of damping has been a developing science in both experimental and analytical senses. Loss factor is widely accepted as one of the major damping indices and is discussed in this research. It is defined as the energy dissipated per radian, normalized by the total mechanical energy.

A. Experimental Methods

Currently used experimental methods to determine damping can be broadly classified into three groups [1–4]:

1) Time-domain free-decay methods use the free transient response of the structure caused by either impulsive excitation or

interrupted steady-state excitation. Damping is obtained from the response-time history. The free-decay method is best suited for lightly damped ($\eta \leq 0.01$) structures (if a directly attached excitation is used) in the low ($f \leq 1000$) and middle ($1000 \leq f \leq 3000$) frequency range.

2) Frequency-domain modal curve-fitting methods determine loss factors at each individual natural mode, using frequency-response function (FRF) data measured from the steady-state response. All modal techniques attempt to match measured data with an analytical model, often by curve-fitting. Modal analysis is best suited for lightly damped structures at low frequencies.

3) The concept of using the power input method to measure structural loss appeared in the late 1970s. However, due to the limitation on the power input method measurement instrumentation and computational capability, it is still being developed. The power input method is not mentioned in the general surveys by Cremer et al. [5], Chu and Wang [6], and Soovere and Drake [7], but it is gradually drawing more attention [2,3,8–10]. Recently, the power input method appears as an alternative method in the general survey by Cremer et al. [11]. Though understanding of the experimental procedure is still developing, the power input method proved to have advantages over the other two methods, because it works at high-frequency ranges ($f \geq 3000$ Hz) and at high damping levels ($\eta \geq 0.1$).

B. Analytical Methods

There has been a need for analytical damping estimation, as shown in the statement by Zhu et al. [12] that "because of the complexity of structural configurations, different materials, interface conditions, joints, etc., damping is usually determined by experiments." When computational capability was limited, closed-form solutions were developed. The usual approach is to start from partial differential equations (PDEs) of motion. The first extensive discussion of damped sandwich beams was given by Ross et al. [13], which was based on a fourth-order partial differential equation. Their solution gave loss factors for infinite-length beams or finite beams with simply supported boundary conditions. DiTaranto [14] derived a sixth-order partial differential equation to describe the motion of the sandwich beam, enabling the analysis of finite-length beams with boundary conditions other than being only simply supported. Mead and Markus [15] refined the theory of DiTaranto by rederiving the partial differential equation and then extended their theory to fixed–fixed beams.

Finite element methods enable the analysis of complex structures as a result of enhanced computational capability. Carne [16] developed a two-dimensional damped beam model using MSC/NASTRAN. Though the shear storage modulus and loss factor of viscoelastic materials are frequency-dependent, they were treated as constants. Johnson et al. [17] proposed the modal strain energy method and developed a three-dimensional plate model using MSC/NASTRAN. The material properties of the middle-damping layer were all treated as real and constant so that a standard normal-modes analysis suffices, followed by an empirical correction to take into account the frequency-dependent material properties. The modal strain energy method is currently widely accepted, and so it is used in this research for the purpose of comparison.

To model the frequency dependency of viscoelastic material properties, several other finite element methods have appeared: namely, the Golla–Hughes–McTavish method [18], the augmenting thermodynamic fields (ATF) method [19], and the anelastic displacement field (ADF) method [20]. These methods augment the usual constant finite element model by introducing internal dissipation coordinates. The results of these augmented finite element methods are concluded to be more accurate than the modal strain energy. However, the additional dissipation coordinates prevent these finite element methods from using commercially available software, which makes them less likely to be used in design.

Current needs in the experimental and analytical estimation of loss factors include 1) a deeper understanding of the experimental procedures of the power input method; 2) application of the power input method to investigate nonuniformly damped structures (e.g., partially covered panels); 3) damping estimation in an extended frequency range (up to 5000 Hz) to meet emerging needs of the transportation industries [21]; 4) an analytical method that can model the frequency dependency of viscoelastic material properties in constrained layer damping and, at the same time, use commercially available finite element software; and 5) comparison of experimental and analytical estimation of loss factors.

II. Experimental Study

A. Experimental Power Input Method

The concept of the power input method to measure the loss factor is based directly on the equation that defines this quantity [8,22,23]:

$$\eta = \frac{P_D}{\omega \cdot E_{\text{Tot}}} = \frac{E_D}{2 \cdot \pi \cdot E_{\text{Tot}}} \tag{1}$$

In a practical measurement, the following conditions exist:

1) The dissipated power is usually converted into heat, which cannot be easily measured. For a steady-state vibration, the dissipated power of the system equals the input power from the excitation. If the structure is driven at a single point, the input power can be estimated from the time-averaged product of the force at the driving point and the velocity at the driving point: $P_D = P_I = \overline{F_f(t) \cdot V_f(t)}$.

2) The total mechanical energy cannot usually be easily measured either, and so it is replaced with twice the kinetic energy: $E_{\text{Tot}} = 2 \cdot E_K = \int_v \rho \cdot \overline{V^2(t)}\, \mathrm{d}v$.

The loss factor expressed in time-averaged terms now becomes

$$\eta = \frac{\overline{F_f(t) \cdot V_f(t)}}{\omega \cdot \int_v \rho \cdot \overline{V^2(t)}\, \mathrm{d}v} \tag{2}$$

Specifically, the input power is

$$\begin{aligned} \overline{F_f(t) \cdot V_f(t)} &= R_{F_f V_f}(0) = \int_0^\infty Re[S_{F_f V_f}(\omega)]\, \mathrm{d}\omega \\ &= \int_0^\infty Re[Y_{ff}(\omega)] \cdot S_{F_f F_f}(\omega)\, \mathrm{d}\omega \end{aligned} \tag{3}$$

and the strain energy is

$$\int_v \rho \cdot \overline{V^2(t)}\, \mathrm{d}v = \int_v \rho \cdot R_{V_i V_i}(0)\, \mathrm{d}v = \int_v \rho \cdot \int_0^\infty S_{V_i V_i}(\omega)\, \mathrm{d}\omega\, \mathrm{d}v \tag{4}$$

But practically, the kinetic energy can only be represented by a finite number of measurements N, representing the response over the whole structure:

$$E_{\text{Tot}} \cong \sum_{i=1}^{N} m_i \cdot \int_0^\infty S_{V_i V_i}(\omega)\, \mathrm{d}\omega$$

Moreover, the preceding equation is obtained by assuming that the excitation frequency varies from zero to infinity; but in reality, the excitation frequency can only vary in a frequency-band $[\omega_1, \omega_2]$. Thus, a frequency-band averaged loss factor is defined as

$$\eta(\omega_C, \Delta\omega) = \frac{\int_{\omega_1}^{\omega_2} Re[Y_{ff}(\omega)] \cdot S_{F_f F_f}(\omega)\, \mathrm{d}\omega}{\sum_{i=1}^{N} m_i \cdot \int_{\omega_1}^{\omega_2} \omega \cdot S_{V_i V_i}(\omega)\, \mathrm{d}\omega} \tag{5}$$

By the mean value theorem for integrals, Eq. (5) can be rewritten as

$$\eta(\omega_C, \Delta\omega) = \frac{(\omega_2 - \omega_1) \cdot Re[Y_{ff}(\omega')] \cdot S_{F_f F_f}(\omega')}{\sum_{i=1}^{N} m_i (\omega_2 - \omega_1) \cdot \omega_i' \cdot S_{V_i V_i}(\omega_i')} \tag{6}$$

where ω' and ω_i' are frequencies in $[\omega_1, \omega_2]$. After simplification, Eq. (6) becomes

$$\eta(\omega_C, \Delta\omega) = \frac{Re[Y_{ff}(\omega')] \cdot S_{F_f F_f}(\omega')}{\sum_{i=1}^{N} m_i \cdot \omega_i' \cdot S_{V_i V_i}(\omega_i')} \tag{7}$$

When $\omega_1, \omega_2 \to \omega_C$ (i.e., $\Delta\omega \to 0$),

$$\lim_{\Delta\omega \to 0} \eta(\omega_C, \Delta\omega) = \frac{Re[Y_{ff}(\omega_C)] \cdot S_{F_f F_f}(\omega_C)}{\sum_{i=1}^{N} m_i \cdot \omega_C \cdot S_{V_i V_i}(\omega_C)} \tag{8}$$

that is,

$$\eta(\omega) = \frac{Re[Y_{ff}(\omega)] \cdot S_{F_f F_f}(\omega)}{\sum_{i=1}^{N} m_i \cdot \omega \cdot S_{V_i V_i}(\omega)} \tag{9}$$

For linear systems, $S_{V_i V_i}(\omega) = |Y_{if}(\omega)|^2 \cdot S_{F_f F_f}(\omega)$, and so the loss factor at a certain frequency becomes

$$\eta(\omega) = \frac{Re[Y_{ff}(\omega)]}{\sum_{i=1}^{N} m_i \cdot \omega \cdot |Y_{if}(\omega)|^2} \tag{10}$$

which is the commonly used expression in the experimental power input method. Each term in Eq. (10) can be measured directly using conventional instruments.

B. Experimental Setup

Aluminum alloy plates are chosen as test articles to simulate aerospace structures (especially, structural skin panels). The damping material used here is viscoelastic-damping polymer 3M Scotch very high bond (VHB) transfer tape F9469PC. Uniformly (fully covered) and nonuniformly (partially covered) damped plates are manufactured. To ensure good bonding between the viscoelastic material and the base structure, surfaces are prepared before attachment and a vacuum is drawn after attachment to apply a pressure of about $1 \cdot 10^5$ Pa.

A shaker hung with bungee cords is used as the excitation, applying pseudorandom loads to excite broadband response. Test articles are suspended by a light and soft spring to simulate free boundary conditions. The other end of the spring is attached to a massive and stiff frame, so that vibrational energy is reflected back to the test article with minimum energy loss at the boundary. Wolf [24] provided a rule-of-thumb for designing suspension systems: to simulate free boundary conditions, the first rigid body mode under the constraint of the suspension should be no more than one-tenth of the first elastic mode. In this research, the vertical translational mode, which is observed to be the most dominant rigid body mode, of the spring-hung plate is measured to be 1.43 Hz, which is much less than one-tenth of the plate's first bending mode (84.7 Hz/10 = 8.47 Hz). The pendulum motion has an even lower frequency (0.75 Hz). Thus, the suspension is assured to be harmless to the results. The response is measured by a Polytec OFV 056 scanning laser vibrometer with a built-in excitation signal generator. The experimental setup is shown in Fig. 1. All tests are done at a room temperature of 25°C (worst case variation: ±1°C).

III. Analytical Study

A. Modeling Sandwich Structures with a Viscoelastic Core

Because of the fact that "the energy in the viscoelastic is almost exclusively linked to shear deformation" [25], the viscoelastic core is modeled as three-dimensional solid elements (HEX/PENT elements in MSC/NASTRAN). Considering the ever-growing computational capacity, the base layer and the constraining sheet are also modeled as three-dimensional solid elements. To avoid shear locking, the length/thickness ratio of solid elements is kept well below 5000 [26]. In this research, the worst case of the length/thickness ratio in the finite element model is 30.85.

Both the shear modulus and the loss factor of the viscoelastic material F9469PC are frequency-dependent, as shown in Fig. 2. But publications in the literature on directly modeling the viscoelastic material properties in constrained layer damping using commercially available finite element software are rarely seen. Belknap [27] pointed out that the complex frequency-dependent shear modulus could be modeled using MSC/NASTRAN by inputting two tabular functions. However, no analytical results were presented. Chang [28] used the same method to model a single degree-of-freedom system to find the resonant frequency. They both referred to the MSC/NASTRAN application manual [29]. This method uses two tabular functions to represent the real and imaginary components of the shear modulus. The equations are

$$TR(f) = \frac{1}{g_{\text{ref}}} \cdot \left(\frac{G_2(f)}{G_{2,\text{ref}}} - 1 \right) \tag{11}$$

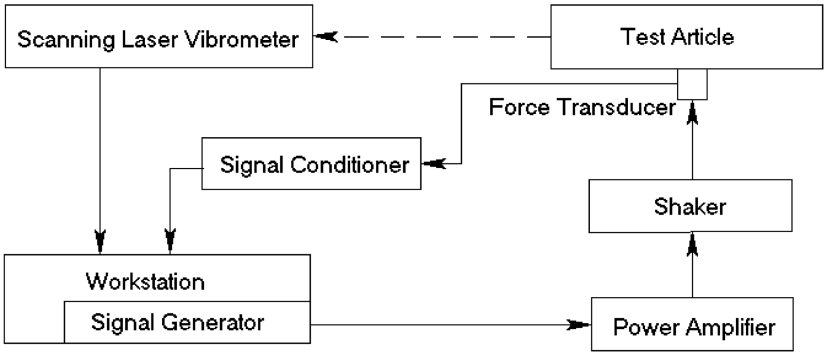

Fig. 1 Experimental setup (lower left: laser vibrometer; lower right: test article with shaker attached).

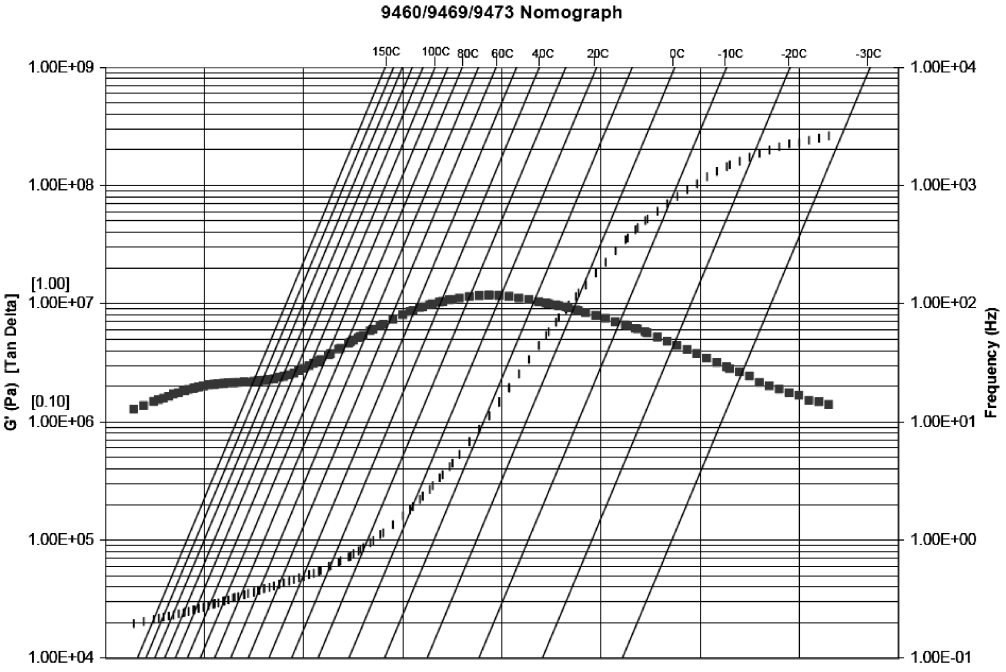

Fig. 2 Nomograph of 3M VHB F9469PC provided by the manufacturer.

$$TI(f) = \frac{1}{g_{\text{ref}}} \cdot \left(\frac{G_2'(f)}{G_{2,\text{ref}}} - g \right) \tag{12}$$

B. Modal Strain Energy Method

In this research, the modal strain energy method is used for the purpose of comparison with the new analytical power input method. The modal strain energy method estimates loss factors of damped structures using a "strain energy ratio" concept:

$$\eta^{(r)} = \sum_{i=1}^{N} \eta_i \cdot \frac{E_i^{(r)}}{E^{(r)}} \tag{13}$$

To obtain the terms in Eq. (13), the material properties of the middle-damping layer are treated as real and constant so that a standard normal modes extraction is applicable. Then, a simple empirical correction to take into account the frequency-dependent material properties is given as [17,26]

$$\eta^{(r)'} = \eta^{(r)} \sqrt{\frac{G_2(f_r)}{G_{2,\text{ref}}}} \tag{14}$$

It is noted that the modal strain energy method tends to overestimate loss factors [30,31]. The error increases with the loss factor of the viscoelastic material and goes to zero as $G_2/G_1 \to 0$ [31]:

$$\frac{\Delta\eta}{\eta} = \frac{\eta^{(r)} - \eta}{\eta} = \left\{ \eta_{\text{vem}}^2 \left[\frac{G_2}{G_1} + \frac{G_3}{G_2} \left(\frac{G_2}{G_1} \right)^2 \right] \right\} \Big/ \left\{ 1 + \frac{G_2}{G_1} + \frac{G_3}{G_2} \left(\frac{G_2}{G_1} \right)^2 \right\} \tag{15}$$

In this research, this error is estimated by the material properties of the viscoelastic material at 5000 Hz ($\eta_{\text{vem}} = 0.9$ and $G_2 = 9 \times 10^6$ Pa) and the material properties of the aluminum ($G_1 = G_3 = 7.45 \times 10^{10}$ Pa). The error (2.36×10^{-8}) turns out to be harmless to the loss factor results in this research.

C. Analytical Power Input Method

The analytical power input method differs from the experimental method in the way that the total mechanical energy is assessed. The finite element method can directly calculate the average strain energy and kinetic energy. Therefore, instead of replacing the total mechanical energy with twice the kinetic energy (as in the experimental power input method), the strain energy and kinetic energy are calculated directly in a frequency-response solution. The total mechanical energy is obtained by the summation of the strain energy (output request ESE) and the kinetic energy (output request EKE).

The input power is represented by the input force and the velocity response of the driving point. It takes an alternative form as [33,34]

$$P_I = \overline{F_f(t) \cdot V_f(t)} = \overline{F_f^2(t)} \cdot Re[Y_{ff}(\omega)] = \tfrac{1}{2} \cdot |F_f(\omega)|^2 \cdot Re[Y_{ff}(\omega)] \tag{16}$$

The driving point mobility can be obtained in finite element solutions. Therefore, with E_{Tot} and P_I both determined, the loss factor can be written as

$$\eta = \frac{\frac{1}{2} \cdot |F_f(\omega)|^2 \cdot Re[Y_{ff}(\omega)]}{\omega \cdot E_{\text{Tot}}(\omega)} = \frac{\frac{1}{2} \cdot |F_f(\omega)|^2 \cdot Re[Y_{ff}(\omega)]}{\omega \cdot [E_K(\omega) + E_S(\omega)]} \tag{17}$$

Thus, as shown in Eq. (17), a new procedure of estimating loss factors is formulated. Instead of making an approximate correction of the constant material properties (as in the modal strain energy method), this analytical method directly takes into account the frequency dependency of viscoelastic material properties in the MSC/NASTRAN direct frequency-response solution, as previously described in Sec. III.A. Examples of loss factor estimation for various damping configurations are presented in later sections.

IV. Validation of the Analytical Power Input Method

To check the validity of the new analytical procedure, a test finite element model is built and the loss factor is computed. A rectangular plate under a point excitation at the center is given arbitrary dimensions, modeled with QUAD elements, assigned with arbitrary material properties, but with a constant loss factor of 0.1. The MSC/NASTRAN frequency-response solution is computed to obtain the mobility function at the driving point, the strain energy, and the kinetic energy at each excitation frequency. Then Eq. (16) is applied

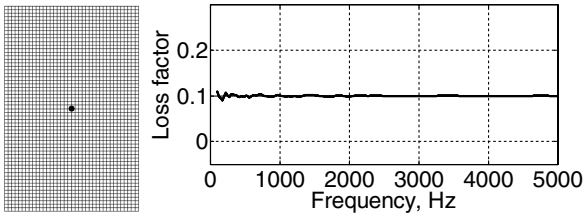

a) b)

Fig. 3 Validation of the analytical power input method: a) finite element model of the plate with the excitation position illustrated and b) calculated loss factor of the plate.

to estimate the loss factor. The results in Fig. 3 show that the new analytical procedure can faithfully evaluate the damping characteristics of the plate. Starting from this point, it is applied for further loss factor estimation.

V. Examples of a Plate with a Nonuniform Constraint Layer Damping Treatment

In this section, experimental and analytical studies on a plate with a nonuniform constrained layer damping treatment are described and discussed. The configuration of the sandwich plate is as shown in Table 1. The partial damping treatment is placed in the central portion of the plate, as shown in Fig. 4.

A. Comparison of Experimental Methods

Results from the experimental power input method are compared with commonly used experimental methods, namely, the free-decay method and the modal curve-fitting method. In the power input method, the plate is divided into 989 portions to minimize the discretization error (the description of the convergence study is omitted, for the purpose of brevity). The driving point position is placed outside of the damped region, as shown in Fig. 4b. Because this plate has a nonuniform damping treatment, the mass m_i in Eq. (10) is not constant over the plate. In the free-decay method, a speaker is used as the excitation. In the modal curve-fitting method, STAR modal analysis software is used.

The comparison in Fig. 5 shows that all three experimental methods yield consistent results, although the power input method gives damping estimation over a broad frequency range, rather than only at several discrete estimations that are basically in the low-frequency range. There are several things to note:

1) The two spikes at 39.4 and 84.7 Hz, respectively, are found to be the first two resonances of the test article/shaker system.

2) The blip around 800 Hz is found to be a test artifact related to stinger length [32].

3) At around 2900 Hz, negative loss factors with very small magnitudes are observed (worst case: −0.003). This is found to be a test artifact that is due to the measurement error of the driving point mobility. As can be seen from Eq. (10), the sign of loss factor is totally determined by the real part of the driving point mobility. In a real test, the laser vibrometer can only measure the front side of the plate instead of the back side where the driving point really is. Thus, if the phase lag between the two sides is greater than 90 deg, a negative real part of the driving point mobility is measured (worst case: -28.4×10^{-6} m/(s · N)), which leads to a slightly negative loss factor.

B. Comparison of Analytical Methods

In this section, the analytical power input method is compared with the commonly used analytical method, namely, the modal strain energy method. Results are shown in Fig. 6. It is observed that at certain frequencies (e.g., 2118, 2913, and 4036 Hz), the modal strain energy method yields abnormally high or low loss factor estimations. A closer look into the corresponding mode shapes reveals the reason. As shown in Fig. 7a, at 2118 Hz, the mode shape involves large displacement in the central damped region. As a result, the ratio of strain energy stored in the viscoelastic material to the strain energy of the whole plate is high, leading to high loss factor estimation in the modal strain energy method. But because the excitation is placed at the node line of this mode, the power input method, which is based on the frequency-response solution, skips this high loss factor. It is the opposite at 2913 Hz: because the excitation is placed at the antinode line of this mode, the power input method "catches" the low loss factor. At 4036 Hz, a low loss factor is estimated by the modal strain energy method, but because the excitation is placed at the node line of this mode, the power input method skips this low loss factor.

The preceding discussion explains why, under a certain excitation, the loss factor result can be different from that predicted by the modal strain energy method. It also demonstrates that a partially covered plate can have very low loss factors in modes for which the strain energy density in the covered region is low.

C. Comparison of the Experimental and Analytical Power Input Methods

The results in Fig. 8 show that the experimental and analytical power input methods yield consistent loss factor estimations below 3100 Hz, which adds further validation to these two methods. The deviation above 3100 Hz is found to be related to the specimen/excitation interaction for this specific experimental configuration:

1) The deviation above 3100 Hz is reduced when a more massive specimen is used, as proved in a later section.

2) Change of stinger lengths returns different loss factor results above 3100 Hz, as shown in Fig. 9.

3) The shaker reaches its first major resonance at about 4500 Hz, as denoted in the shaker specification.

For experimental loss factor estimation in a high-frequency range, it is recommended to use a specimen/shaker armature combination that has a weight ratio above three (based on practice), a shaker with a higher resonance frequency, and a stinger with medium length (3 cm $\leq L \leq$ 6 cm).

Table 1 Description of the plate with a nonuniform damping treatment

	Material	Dimensions, mm	Weight, g
Base layer	CLAD 2024-T3	349.0 × 202.9 × 1.60	311.2
Damping layer	3M F9469PC at 25°C	202.9 × 101.9 × 0.127	2.63
Constraining sheet	CLAD 2024-T3	202.9 × 101.9 × 0.508	29.1

Table 2 Description of the plate with a uniform damping treatment

	Material	Dimensions, mm	Weight, g
Base layer	5052-H34	347.0 × 201.0 × 3.06	572.1
Damping layer	3M F9469PC at 25°C	347.0 × 201.0 × 0.127	8.9
Constraining sheet	CLAD 2024-T3	347.0 × 201.0 × 0.508	29.1

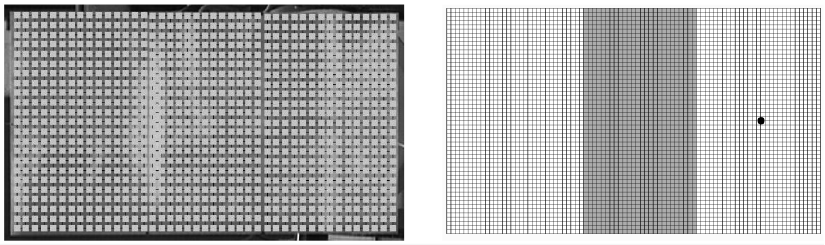

a) b)

Fig. 4 The plate with a nonuniform damping treatment: a) the plate as a test article with scanning points defined and b) the plate as a finite element model with the excitation position illustrated.

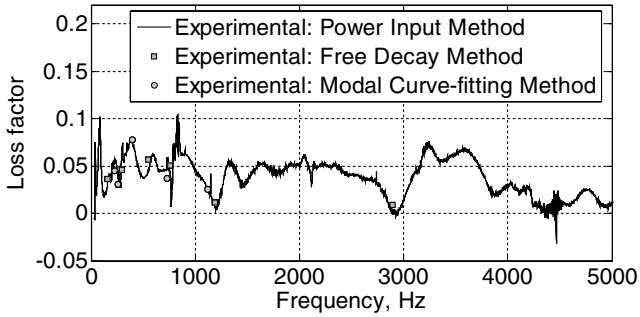

Fig. 5 Loss factor results by different experimental methods.

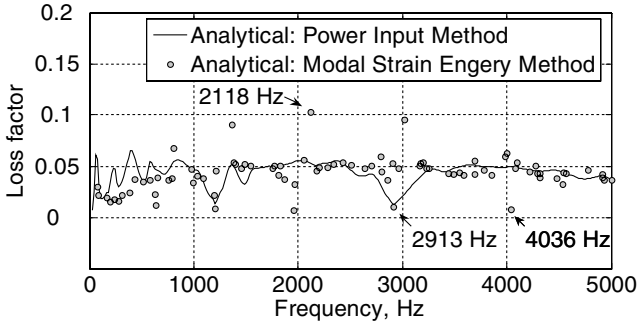

Fig. 6 Loss factor results by different analytical methods.

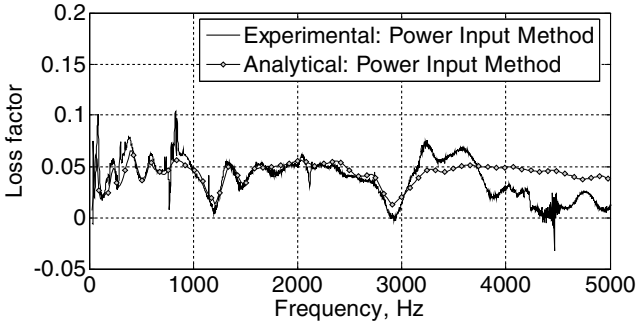

Fig. 8 Loss factor results by the experimental and analytical power input method.

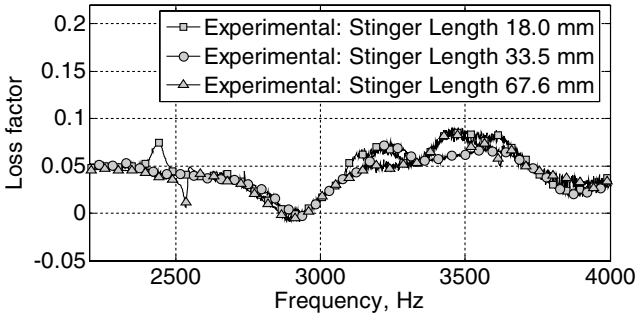

Fig. 9 Loss factor results obtained using different stinger lengths.

VI. Examples of a Plate with a Uniform Constraint Layer Damping Treatment

This sandwich plate is intentionally made more massive than the plate, with a nonuniform damping treatment to suppress the specimen/excitation interaction. The plate is described in Table 2 and Fig. 10. The same data reduction procedure is used (as explained in Sec. V).

The following conditions can be observed in Fig. 11:

1) The specimen/excitation interaction above 3100 Hz, as shown in the previous partially covered plate, is effectively improved because of the increased mass of this specimen.

2) The loss factor of this uniformly damped plate varies less dramatically with frequency than does the loss factor of the nonuniformly damped plate. This is due to the fact that the fully

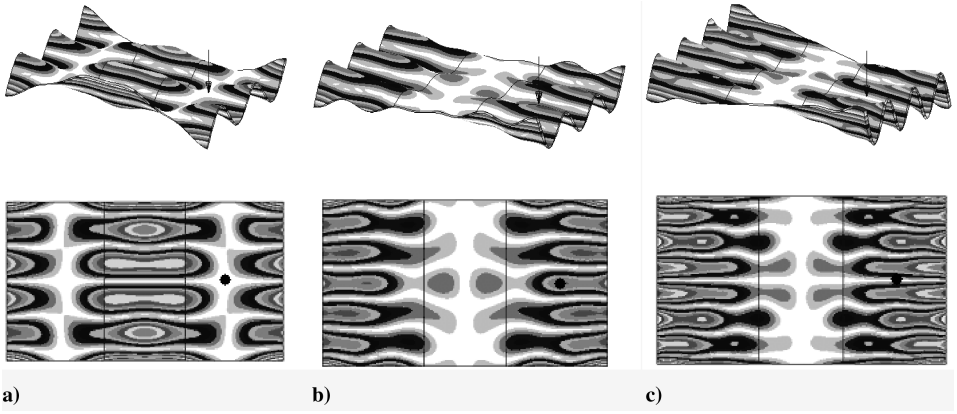

a) b) c)

Fig. 7 Selected mode shapes of the plate with a nonuniform damping treatment: a) 2118 Hz, b) 2913 Hz, and c) 4036 Hz.

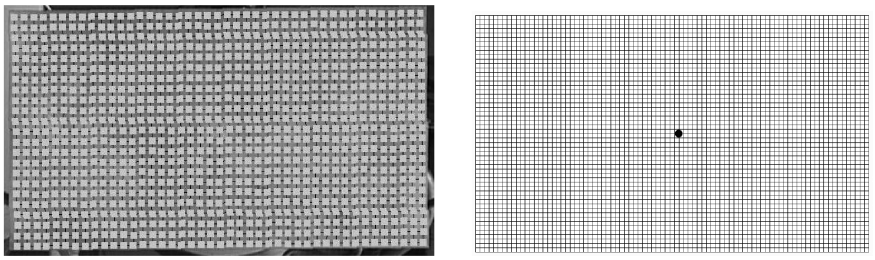

a) b)

Fig. 10 The plate with a uniform damping treatment: a) the plate as a test article with scanning points defined. b) the plate as a finite element model with the excitation point illustrated.

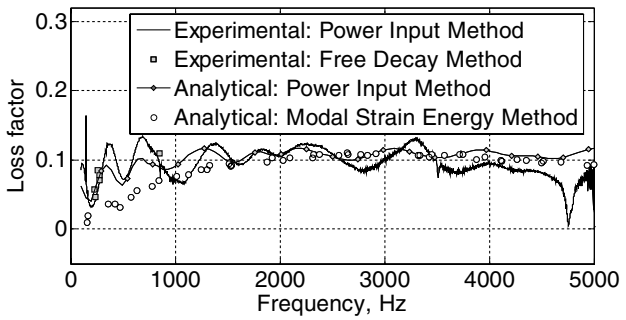

Fig. 11 Experimental and analytical loss factor results of the plate with a uniform damping treatment.

covered plate cannot have modes in which the strain energy density is greatest in the uncovered portions.

3) The analytical and experimental power input methods give satisfactory agreement, except where instrumental difficulties arise at about 4750 Hz.

4) In the frequency range below 1000 Hz, the results are as follows:

a) The experimental power input method and free-decay method agree well at the limited number of frequencies at which the free-decay method results suffice (efforts have been made to obtain loss factors around the 500 Hz range using the free-decay method, but no clean decay history was found).

b) The analytical power input method appears to give a more consistent estimation with the experimental methods (the power input method and free-decay method) than with the modal strain energy method.

c) All four methods show the trend of diminishing loss factor as the frequency decreases to the lowest mode, considering the fact that, for the power input methods (both experimental and analytical ones), certain modal density is needed to reduce the estimation error [2]. In other words, the power input methods give acceptable loss factor estimation only after the first resonance.

VII. Conclusions

In this research, results of experimental and analytical methods of loss factor estimation are presented, compared, and discussed. Major work includes the following:

1) A new analytical power input method is proposed, validated, and applied for sandwich plates with various damping configurations. Both the analytical power input method and the modal strain energy method yield consistent results with the experimental power input method. But the consistency appears to be subject to details of the experimental configuration (e.g., shaker and stinger properties).

2) In frequency ranges for which other commonly used experimental methods apply (below 3000 Hz), the experimental power input method yields consistent results with those other experimental methods.

3) The frequency dependency of the viscoelastic materials is directly taken into account in the finite element model using MSC/NASTRAN.

4) For the specific experimental configuration in this research, instrumentation causes of difficulties in loss factor measurement in the high-frequency range are identified and recommendations are made.

Possible sources of the estimation error can be 1) specimen/excitation interaction, as shown in Sec. V; 2) defects caused in the specimen manufacturing process (e.g., debonding of the viscoelastic materials and unsquareness of test specimens); 3) approximations in the finite element modeling; 4) quality variation of the viscoelastic materials; and 5) drift of the room temperature during the test ($\pm 1^{\circ}$C).

To design a trustable experiment using the experimental power input method, several things need to be noted:

1) The specimen should be divided into enough portions so that the kinetic energy can be faithfully measured. In other words, discretization error should be avoided.

2) A specimen/shaker armature combination should have a weight ratio above three (based on practice). In other words, the shaker should not be too big for the test articles, so that the shaker will not dominate the vibration.

3) The shaker should have a higher resonance frequency than the upper limit of the interested frequency range. In other words, as long as the shaker is powerful enough to drive the specimen, a small shaker is preferred.

4) Very short stinger lengths should be avoided.

To build a trustable finite element model so that the analytical power input method can be used, two things need to be noted:

1) Discretization error should be avoided so that the total energy can be faithfully calculated.

2) The length/thickness ratio of solid elements should be kept below 50, to avoid shear locking.

For more complex and built-up structures, the analytical power input method will not raise particular difficulties. But the experimental method would require scanning surfaces individually and rotating the specimen/shaker accordingly if the test article does not have a simple two-dimensional shape (e.g., a T-shaped structure or a cylinder). Then scans should be combined to obtain the total kinetic energy. However, for an E-shaped structure, using the scanning laser vibrometer to obtain loss factors will be impractical, because it cannot really see the middle panel. Manually positioned accelerometers may be used instead.

References

[1] Jacobsen, Finn, "Experimental Determination of Structural Damping," *Proceedings of the Nordic Acoustical Meeting '86*, Acoustical Society of Finland, Espoo, Finland, 1986, pp. 361–364.

[2] Carfagni, M., and Pierini, M., "Determining the Loss Factor by the Power Input Method (PIM), Part 1: Numerical Investigation," *Journal of Vibration and Acoustics*, Vol. 121, July 1999, pp. 417–421.

[3] Carfagni, M., and Pierini, M., "Determining the Loss Factor by the Power Input Method (PIM), Part 2: Experimental Investigation with Impact Hammer Excitation," *Journal of Vibration and Acoustics*, Vol. 121, July 1999, pp. 422–428.

[4] Bloss, B., and Rao, M. D., "Measurement of Damping in Structures by the Power Input Method," *Experimental Techniques*, Vol. 26, Part 3, May 2002, pp. 30–32.

[5] Cremer, L., Heckl, M., and Ungar, E., *Structure-Borne Sound*, 1st ed., Springer–Verlag, Berlin, 1973.
[6] Chu, F. H., and Wang, B. P., "Experimental Determination of Damping in Materials and Structures," *Damping Application for Vibration Control*, edited by P. J. Torvik, American Society of Mechanical Engineers Winter Annual Meeting, Chicago, 1980, pp. 113–122.
[7] Soovere, J., and Drake, M. L., "Aerospace Structures Technology Damping Design Guide, Vol. 1: Technology Review," U.S. Air Force Wright Aeronautical Laboratories, Rept. AFWAL-TR-84-3089, Wright–Patterson AFB, 1985.
[8] Jacobsen, F., "Measurement of Structural Loss Factors by the Power Input Method," Acoustics Lab., Technical Univ. of Denmark, Rept. 41, 1986.
[9] Plunt, J., "Power Injection Method for Vibration Damping Determination of Body Panels with Applied Damping Treatments and Trim," *S.A.E. Transactions*, Vol. 100, No. 6, Society of Automotive Engineers, New York, May 1991, pp. 1563–1571.
[10] Carfagni, M., Citti, P., and Pierini, M., "Determining Loss Factor Using the Power Input Method with Shaker Excitation," *Proceedings of the 16th International Modal Analysis Conference*, Society for Experimental Mechanics, Bethel, CT, 1998, pp. 585–590.
[11] Cremer, L., Heckl, M., and Petersson, B. A. T., *Structure-Borne Sound*, 3rd ed., Springer–Verlag, Berlin, 2005.
[12] Zhu, G. H., Crocker, M. J., and Rao, M. D., "Data Processing and Accuracy Analysis of Damping Measurement," *Journal of the Acoustical Society of America*, Vol. 85, No. 1, 1989, pp. 171–177.
[13] Ross, D., Ungar, E. E., and Kerwin, E. M., Jr., "Damping of Plate Flexural Vibrations by Means of Viscoelastic Laminae," *Structural Damping*, edited by J. E. Ruzicka, American Society of Mechanical Engineers, New York, 1959, pp. 49–88.
[14] DiTaranto, R. A., "Theory of Vibratory Bending for Elastic and Viscoelastic Layered Finite-Length Beams," *Journal of Applied Mechanics*, Vol. 32, No. 6, Dec. 1965, pp. 881–886.
[15] Mead, D. J., and Markus, S., "The Forced Vibration of a Three-Layer Damped Sandwich Beam with Arbitrary Boundary Conditions," *Journal of Sound and Vibration*, Vol. 10, No. 2, 1969, pp. 163–175.
[16] Carne, T., "Constrained Layer Damping Examined by Finite Element Analysis," *Proceedings of the University of Texas*, 12th Annual Technical Meeting of the Society of Engineering Science, Univ. of Texas, Austin, TX, 1975, pp. 567–576.
[17] Johnson, C. D., Kienholz, D. A., and Rogers, L. C., "Finite Element Prediction of Damping in Beams with Constrained Viscoelastic Layers," *Shock and Vibration Bulletin*, No. 50, Part 1, 1981, pp. 71–82.
[18] McTavish, D. J., and Hughes, P. C., "Finite Element Modeling of Linear Viscoelastic Structures: The GHM Method," *Proceedings of the 33rd AIAA/ASME/ASCE/AHS/ASC Structures, Structural Dynamics, and Materials Conference*, AIAA, Washington, D.C., 1992, pp. 1753–1763.
[19] Lesieutre, G. A., and Mingori, D. L., "Finite Element Modeling of Frequency-Dependent Material Damping Using Augmenting Thermodynamic Fields," *Journal of Guidance, Control, and Dynamics*, Vol. 13, No. 6, 1990, pp. 1040–1050.
[20] Lesieutre, G. A., and Bianchini, E., "Time Domain Modeling of Linear Viscoelasticity Using Anelastic Displacement Fields," *Journal of Vibration and Acoustics*, Vol. 117, No. 4, 1995, pp. 424–430.
[21] Plunt, J., "Predictability of Mid- And High-Frequency Dynamic Properties of Industrial Product," *Eighth International Conference on Recent Advances in Structural Dynamics*, Institute of Sound and Vibration Research, Southampton, England, U.K., 2003.
[22] Ranky, M. F., and Clarkson, B. L., "Frequency Average Loss Factors of Plates and Shells," *Journal of Sound and Vibration*, Vol. 89, No. 3, 1983, pp. 309–323.
[23] Bies, D. A., and Hamid, S., "In Situ Determination of Loss and Coupling Loss Factors by the Power Injection Method," *Journal of Sound and Vibration*, Vol. 70, No. 2, May 1980, pp. 187–204.
[24] Wolf, J. A., Jr., "The Influence of Mounting Stiffness on Frequencies Measured in a Vibration Test," Society of Automotive Engineers Paper 840480, 1984.
[25] Plouin, A., and Balmes, E., "Steel/Viscoelastic/Steel Sandwich Shells Computational Methods and Experimental Validations," *Proceedings of SPIE: The International Society for Optical Engineering*, Vol. 1, No. 4062, 2000, pp. 384–390.
[26] Johnson C. D., and Kienholz, D. A., "Finite Element Prediction of Damping in Structures with Constrained Viscoelastic Layers," *AIAA Journal*, Vol. 20, No. 9, Sept. 1982, pp. 1284–1290.
[27] Belknap, F. M., "Vibration Reduction of Composite Structures Using Constrained Layer Damping Techniques," *32nd AIAA/ASME/ASCE/AHS/ASC Structures, Structural Dynamics, and Materials Conference*, Part 3, AIAA, Washington, D.C., 1991, pp. 2391–2396; also AIAA Paper A91-31826 12-39.
[28] Chang, Y., "Linear Viscoelastic Material Properties in MSC/NASTRAN with Power Spectral Density Input," *MSC 1992 World Users' Conference Proceedings*, Vol. 2, MSC Software Corp., Paper 48, Santa Ana, CA, 1992.
[29] Anon., "MSC/NASTRAN Application Manual," MacNeal Schwendler Corp., Santa Ana, CA, 1983, Sec. 2.11.
[30] Torvik, P. J., and Runyon, B., "On the Application of the Method of Modal Strain Energy to the Determination of Loss Factors for Damped Sandwich Beams," *Proceedings of the 75th Shock and Vibration Symposium* [CD ROM], Shock and Vibration Information Analysis Center, Falls Church, VA, 2004.
[31] Torvik, P. J., and Runyon, B., "Observations on the Accuracy of Finite Element Predictions of Constrained Layer Damping," *10th National Turbine Engine High Cycle Fatigue Conference*, Universal Technology Corp., Dayton, OH, 2005.
[32] Liu, W., and Ewing, M., "Experimental and Analytical Estimation of Loss Factors by the Power Input Method," AIAA Paper 2006-2233, 2006.
[33] De Langhe, K., and Sas, P., "An Experimental-Analytical SEA Identification and Applied Validation Criteria for a Box Type Structure," *Proceedings of the 19th International Modal Analysis Conference*, International Conference on Noise & Vibration Engineering, Leuven, Belgium, 1994.
[34] Brown, K. T., and Norton, M. P., "Some Comments on the Experimental Determination of Modal Densities and Loss Factors for Statistical Energy Analysis Applications," *Journal of Sound and Vibration*, Vol. 102, No. 4, 1985, pp. 588–594.

E. Livne
Associate Editor